Melting of Metallic Electrodes and Their Flowing Through a Carbon Nanotube Channel within a Device

Rujia Zou, Zhenyu Zhang, Qian Liu, Kaibing Xu, Aijiang Lu, Junqing Hu, Quan Li, Yoshio Bando, and Dmitri Golberg*

The performances of integrated circuits within electronic devices have been steadily improved over the last few decades through miniaturizing the transistors and narrowing the interconnecting wires. Compared to the traditional copper wires, due to outstanding electronic properties, metallic carbon nanotubes (CNTs) are a promising material for such interconnects in the future electronic devices.[1] Thus, considerable researches have been actively done on the CNT interconnecting wires in vertical[2] and horizontal configurations for the devices.[3] Much effort has been made to realize a reliable electrical contact between the CNT and contacting metallic electrodes (e.g., gold) and to evaluate their structural integrity within specific devices.[4] Recently, in-situ transmission electron microscope (TEM) technique has been developed for establishing a simple electronic device based on an individual nanostructure, and thus real-time probing its electrical performances inside TEM under nearly atomic resolution has become possible. Several types of metal (such as copper,[5] iron,[6] or tin[7]) or compound (such as Fe_3C,[8] CuI,[9] or ZnS[10])-filled CNT based devices were engineered and established by contacting such a CNT to two opposite metallic tips (electrodes) forming a circuit, and then their performances were electrically probed, and structurally, chemically and thermally analyzed. However, the foreign material filled CNTs involved in these works are always synthesized by physical encapsulation or chemical encapsulation (such as capillary adsorption[11] or chemical vapor deposition method[5–10]) in advance before the observation and in-situ manipulation in the TEM. In addition, little is known about Joule heating-induced melting of metallic electrodes in the CNT based devices that may result in a flow of the liquid electrode material through the CNT channel and strongly affect the electrical performances. So, more studies of these fundamentally interesting and practically important effects closely related the CNT based devices are required.

Herein, we present a time-resolved, high-resolution in-situ TEM analysis of the real electrical performances of the electronic devices based on a two-terminal CNT. An individual pure multiwalled CNT (without any foreign fillings inside its tubular channel) was exploited directly as an interconnecting wire; as-established device includes this CNT contacted by two noble metal electrodes forming a circuit. During the study three particularly important phenomena were discovered: i) metallic electrode materials, e.g., Au, Ag, and Pt, melt and flow through the CNT channel within these devices; ii) electrical performances of such devices are strongly affected by this process, often causing electrical shortening and even breakdown of pre-established devices; iii) destruction of the CNT devices may be avoided by selecting a CNT with a right length and controlling a bias. In addition, systematic dynamics analysis about the effects of the electromigration and thermomigration on the mass transportation of the liquid Au filling inside the CNT was carried out. This study demonstrates that the electrode melting and its material flow through the CNT channel may be one of the main reasons accounting for the unstable performance and the electrical breakdown and even catastrophic failure of the established CNT-based devices. Needless to say, the observed effects are of importance for the CNT-based devices.[12]

Multiwalled CNTs were grown by a chemical vapor deposition process.[13] As grown CNTs have a diameter of 30–50 nm, and a wall thickness of ~5 nm which is composed of regularly ordered graphitic layers. The experimental setup for making a CNT-based device is depicted in the inset of **Figure 1**a, which involves a CNT contacted by two Au electrodes (0.25 mm in diameter) establishing a circuit via the sidewall-contact configuration using a piezo-driven scanning tunneling microscope (STM)-transmission electron microscope (TEM) holder (Nanofactory Instruments AB). The detailed procedure can be found in Figure S1 (Supporting Information). An inset in Figure 1b is a TEM image showing that the CNT is connected between the movable Au wire (left-hand side, anode) and the fixed Au tip (right-hand side, cathode) through its sidewall. The CNT has a diameter of ~30 nm, a wall thickness of ~5 nm and a length of ~500 nm. Applying a voltage between the two electrodes drives a flowing current through the device; the electrical properties were continuously measured for evaluating its performance. For realizing good Ohmic contacts between

Dr. R. J. Zou, Mr. Z. Y. Zhang, Q. Liu,
K. B. Xu, Prof. J. Q. Hu
State Key Laboratory for Modification of Chemical Fibers and Polymer Materials
College of Materials Science and Engineering
Donghua University
Shanghai 201620, China
E-mail: hu.junqing@dhu.edu.cn
Dr. A. J. Lu
Department of Applied Physics
Donghua University
Shanghai 201620, China
Prof. Q. Li
Department of Physics
The Chinese University of Hong Kong
Shatin, New Territory, Hong Kong
Prof. Y. Bando, Prof. D. Golberg
International Center for Materials Nanoarchitectonics (MANA)
National Institute for Materials Science (NIMS)
1-1 Namiki, Tsukuba, Ibaraki 305-0044, Japan

DOI: 10.1002/adma.201300257

the CNT and the Au electrodes, a bias was gradually increased to promote Joule heating at the interfaces of the CNT/Au electrodes owing to a contact resistance. When the local temperature increased and exceeded the melting point of Au, a tight contact between the CNT and the electrodes was realized via a sort of soldering.[10,14a,15] Due to a good thermal conductivity of macroscopic metal electrodes, the thermal distribution is radial on the bulk metal electrodes,[14] i.e., from the hottest place at the contact points between the CNT and the Au electrodes to the common temperature on the other positions on the electrodes. So, compared with the contact points, the other positions on the bulk electrodes can not melt. The initial *I-t* curve has strong shape variations and illustrates a gradual evolution of the device from its almost insulating state to a clear Ohmic-type device, Figure 1a. While applying an initial bias of 3000 mV, a current in a period of 0–4 min was measured to be as low as several nA, suggesting a high resistance (~10^6 kΩ) of as-made CNT device, Figure 1b (curve 1). Then it abruptly increased to tens of thousands nA after 6 min. At this point, the corresponding *I–V* curve (Figure 1b, curve 2) reveals a fingerprint of the good Ohmic contact between the CNT and the metal (a resistance of 44.89 kΩ was measured for this CNT device). As reported earlier, when an electrical current flows through the CNT circuit under a constant voltage, Joule heating causes the temperature increase on it.[10,14b,15] It is found here that such a temperature increase on the CNT indeed results in gradual lowering of the system resistance and a gradual increase of the current flowing through it (Figure 1b, curves 2–5, see method 1 in Supporting Information). Notably, after a few minutes of biasing, a thermal equilibrium between a thermal gain and a thermal loss on the CNT has been achieved, and at this time the resistance of the device is stabilized. Then, we observed melting of the Au electrode and its initial filling into the CNT channel, Figure 1c. An upper-right inset shows that the Au filling has not taken place at the beginning of biasing (1.5 V). As the current through the device is kept stable at ~43.85 μA (Figure S2), it is believed that the temperature on the CNT is also nearly stable due to reaching thermal equilibrium. The resistance of this device is determined to be ~35.24 kΩ from the *I–V* curve (Figure 1d, curve 1). After ~10 min, due to Joule heating, the Au electrode melts close to the CNT/Au interface and the melt starts to enter the CNT channel along the direction opposite to the current flow. (It is hard to measure the exact temperature at the CNT/Au interface under biasing, but it is supposed to reach the Au melting point of ca. 1063 °C under the present experimental conditions). The *I–V* curve suggests lowering resistance of this device to ~29.97 kΩ (Figure 1d, curve 2). Compared with the former resistance, a decrease of 5.27 kΩ is attributed to a short Au-filling inside the CNT channel, as this short metallic segment obviously participates in the electron transport of the device. After biasing was terminated, the CNT was retracted, leaving the freshly filled material solidified onto the Au tip (the lower-right inset of Figure 1c), as suggested by a high-magnification TEM imaging (the upper-left inset of Figure 1c).

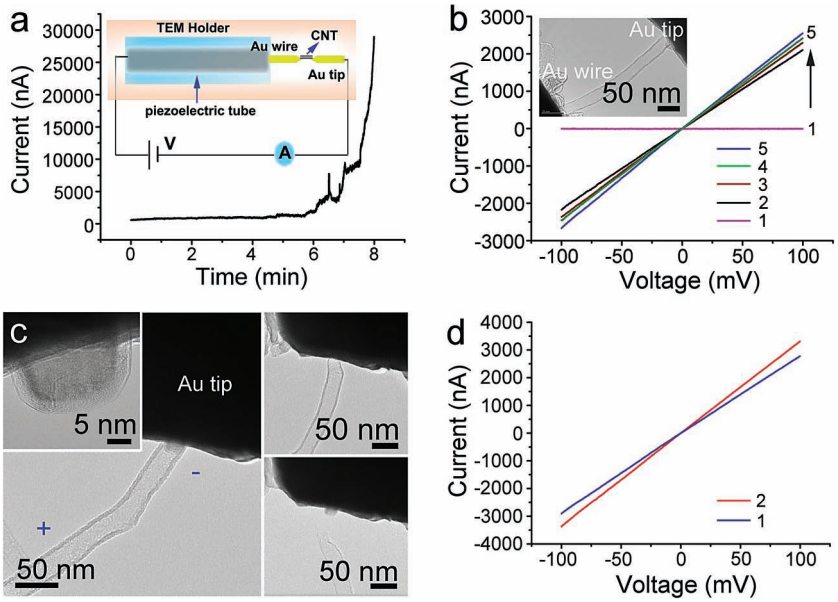

Figure 1. (a) A current flows through a CNT device made by establishing an Au-CNT-Au circuit via the sidewall-contact configuration; the inset shows the experimental setup. (b) *I–V* curves taken from the device under a temperature increase on it; the inset is a TEM image showing the contacts made under this configuration. (c) A TEM image illustrating the Au electrode melting at the CNT/Au interface and the Au melt starting to flow into the CNT channel; the upper-right inset confirms that the Au filling does not exist at the beginning of biasing; the lower-right and the upper-left insets show the remaining Au nanoparticle resting on the Au electrode after the CNT was pulled backward. (d) *I–V* curves recorded from the original CNT device and the Au filled-CNT device.

Systematic study was performed to investigate the Au flowing process within this CNT device using real-time video recording, **Figure 2**. After applying a positive bias of 1.5 V to the Au wire, which, thus, served as an anode electrode, a current through the circuit stabilized at ~27.46 μA. The temperature at the Au-CNT sidewall-contacts rose high and the Au electrodes began to melt. After ~9 min, more Au was melted, and then the melt flew into the CNT channel along the direction opposite to the current flow (see Movie 1), compared with the original state of this CNT end and the Au electrode, Figure 2a. Clearly, dark contrast and nearly hemispherical metal tip indicates that Au is liquid in the CNT. Figure 2b gives a series of real-time video frames illustrating the entire liquid Au flowing process inside the CNT channel. After putting a bias of 1.5 V over 2 min, a considerable amount of molten Au was produced that continuously flew down the CNT, from the contact side to its mid-portion, at a longitudinal speed of 1.35 nm s^{-1} (~70 nm within 52 s). In the following 60 s of biasing, the flow speed slightly decreased to ~1.05 nm s^{-1}. After another 65 s of biasing, the flowing melt front almost reached the CNT middle region, and then did not flow anymore, Figure 2c. Instead, the Au filling front slightly vibrated inside the CNT, which may be caused by electron beam irradiation and mechanical noise. The transported mass of the

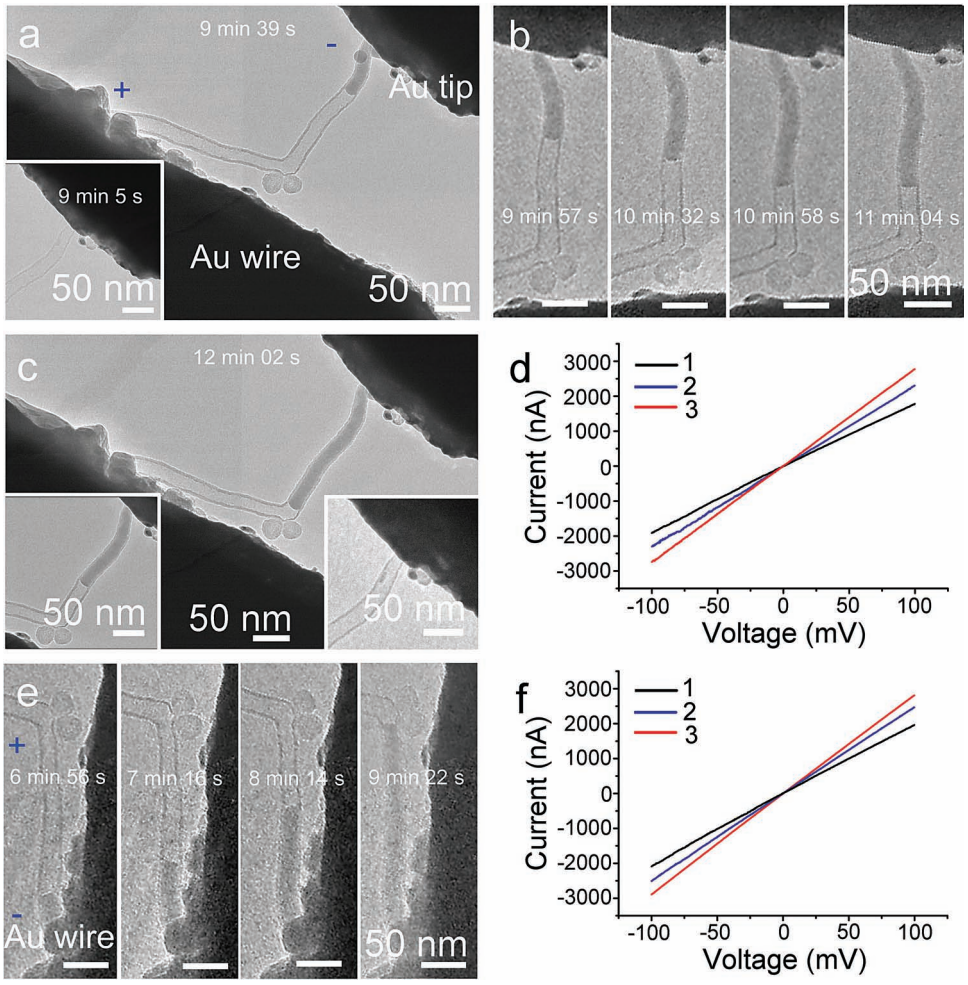

Figure 2. (a) A TEM image shows that the molten Au electrode enters the CNT channel through the device; the inset illustrates the original state of the CNT end contacting Au electrode. (b) A series of four TEM images demonstrate that the liquid Au flows into the tube and (c) reaches the middle of the CNT upon applying a positive bias, and the lower-left and the lower-right insets in (c) display that liquid Au filling moves back into the CNT channel as the bias slightly increases, finally leaving the CNT totally empty, again. (d) *I–V* curves are taken from the CNT device without Au filling (curve 1), with Au filling occupying about 1/4 of the channel length (curve 2) and a half of the tube cavity (curve 3), respectively. (e) A series of consecutive TEM images confirm that the melt flows through the tube and reaches the middle portion of the CNT upon applying a negative bias. (f) *I–V* curves are taken from the CNT device without Au filling (curve 1), with Au filling occupying about 1/4 of its length (curve 2) and a half of its cavity (curve 3), respectively.

molten Au inside the CNT was calculated to be ~0.721 fg (1 fg = 10^{-15} g). The corresponding *I–V* curves, Figure 2d, were taken from the device with the different amount of Au filling in the CNT, i.e., no Au filling (curve 1), Au filling occupying about 1/4 of its length (curve 2), and a half of the CNT cavity (curve 3). Here, the device resistance in curve 3 is as low as ~36.12 kΩ, which is lower than that for the unfilled CNT device (~54.03 kΩ) (curve 1). The resistance of both the empty and filled CNT based device can be comparable with the previous reports by using STM-TEM holder.[6b,16] Obviously, the metal Au filling can serve as a part of the current pathway within the device (Au filling also was characterized by EDX, Figure S3). And thus the electrical conductivity of the as-made device is improved, which agrees with the relevant observations for other metal-filled CNT systems.[6b,17] Interestingly, as positive bias was increased to 1.6 V, the melt began to flow backward and out of the CNT along the direction of the current flow. After ~8 s, the filling was shorten to 3/5 of its original length, and then did not move, as shown in the lower-left inset of Figure 2c (see Movie 2). When a positive bias was increased to 1.9 V, the liquid Au completely escaped from the CNT after ~25 s, leaving the CNT totally empty again, as shown in the lower-right inset of Figure 2c. Comparatively, when the device was applied a negative bias, similar phenomenon was demonstrated (see method 2 in Supporting Information). Applying –1.5 V, Au electrode melting and then Au melt flowing in the opposite direction of the current flow inside CNT were observed, and after 6 min the Au melt flowing was almost terminated at the middle of this CNT, Figure 2e. The *I–V* curves, Figure 2f, taken from the device without Au filling (curve 1), with Au filling occupying about 1/4 of its length (curve 2) and a half of its cavity (curve 3), respectively, inside the CNT, suggest that electrical performances are obviously affected by this Au filling process. When a bias increased to –1.9 V, the molten Au also began to flow backward inside the

CNT and finally completely escaped from the CNT. The flowing processes inside the CNT channel can be repeated in an interval several times as long as the electron beam is weak enough and the irradiation-induced destruction of the CNT is minimized. We further verified these results by constructing the Ag-CNT-Ag (Figure S4) and Pt-CNT-Pt circuits (Figure S5). Although the mass transport on or inside the nanotubes has been previously described for a variety of materials,[5–10,18] the current work may shed an additional light on this interesting phenomenon.

It is reasonable to deduce that continuous flowing of the liquid Au through the whole CNT channel may shorten as-established circuit, and sharply reduce the device resistance, even causing electrical breakdown of the device. **Figure 3**a shows a short CNT (length: ~60 nm) connected by two Au electrodes for making a CNT device. After applying a bias of –1.5 V for ~7 min, Au electrode melts and begins to flow into the CNT along the opposite direction of the current flow; after additional ~2 min, the flow front of this Au filling reaches the middle of the tube, Figure 3b, and then the Au filling easily passes through the middle point and rapidly moves to the counterpart Au electrode, and thus completely fills the CNT, Figure 3c. At this time, due to a very low resistance of the liquid Au column in the CNT, the current through this device suddenly increases (from –43.37 μA) and exceeds the detection limit of the STM-TEM setup, resulting in electrical shortening of the established Au-CNT-Au circuit. (According to the conductivity of liquid Au, the current value is estimated to be up to ~1.52 A, corresponding to a current density of ~4.78×10^{12} A m^{-2}, as Au melt fully fills the CNT.) However, after another ~ 9 s, the liquid Au filling transferred completely from this Au electrode to the other, leaving a completely empty CNT again, Figure 3d. At this time, the current value of this device is~ –44.12 μA, which indicates that the electrical performance of this device does not notably change. Interestingly, as this bias voltage was kept for another ~5 min, the above described transfer processes start again, and proceed similarly (see Movie 3). This behavior resembles the initially designed approach for a CNT as a water "pump" for the water transfer,[12a,19] except that the liquid Au is substituted for water here. It is believed that via this CNT pumping more and more amount of molten Au will transfer from one electrode to the other if the bias voltage is kept for a long time. A time series of consecutive TEM images, Figures 3e–h, show a flow of liquid Au through a long CNT (length: ~250 nm) within another device. Biasing a voltage of 1.7 V, within a long period, the Au melt cannot flow into the CNT at all. While this voltage was adjusted to 1.4 V, the Au molten can rapidly pass through the CNT, and a mass transfer from one Au electrode to the other (see Movie 4) takes place. Similarly, when this CNT was completely filled by the Au melt, a current value through this device also far exceeded the detection limit of the STM-TEM setup. So, though melting of Au electrodes and Au flowing through a CNT channel within the device may cause the electrical shortening of the CNT circuits and electrical breakdown of the CNT based devices, it is expected that by selecting a right length of the CNT and optimizing an applied voltage it can enable a safe electrical performance of the CNT-based devices.

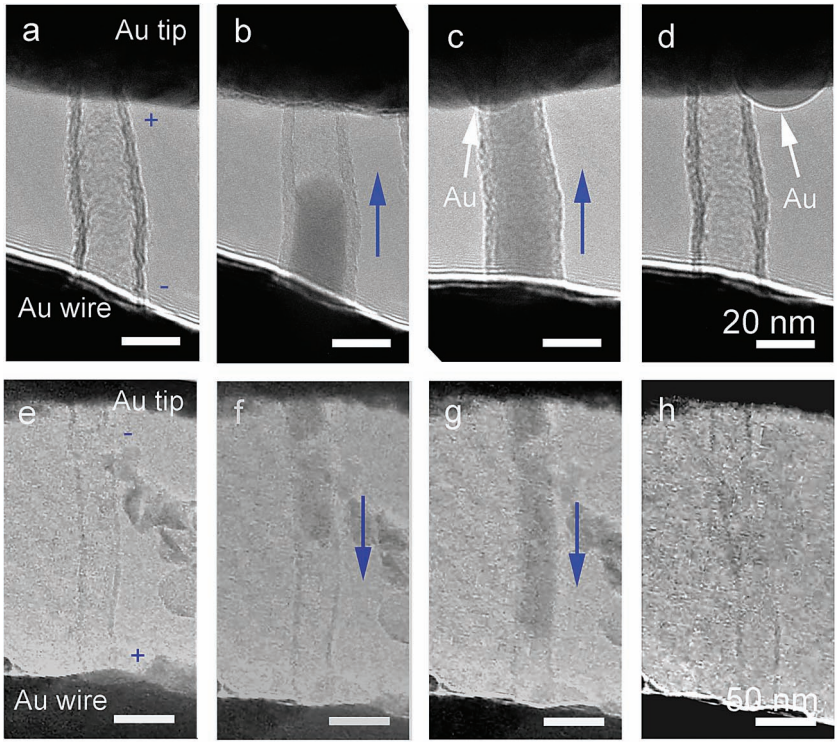

Figure 3. Consecutive TEM images show the absence of the Au filling in a short CNT: the beginning of biasing (a), Au filling flow passing through the middle (b), reaching the counterpart Au electrode and thus completely filling the CNT (c), and a complete transferring from one Au electrode to the other, leaving the CNT empty again (d). (e-h) A time series of consecutive TEM images reveal an Au liquid mass transport process inside a long CNT from one Au electrode to the other.

Flowing of the molten Au through the CNT channel might be due to many effects such as thermomigration,[15] electromigration,[20] capillarity,[21] thermal expansion, frictional force, and shell-shrinkage.[22] Due to a small contribution to the mass transport, the effects of capillary, thermal expansion, frictional force, and shell-shrinkage can be excluded (see method 3 in Supporting Information and Figure S6). So, for a two-terminal connected CNT, there are mainly two liquid transport mechanisms. One is thermomigration, i.e., a temperature gradient pushes the Au melt from the hotter spot to the cooler spot; the other is electromigration, i.e., the current induces the Au melt to follow the direction of the electron flow. We have developed a qualitative model that accounts for the above transport dynamics. In this model, two forces of electromigration force ($F_{electro}$) and thermomigration force (F_{thermo}) impose on the liquid Au filling in the CNT, **Figure 4**a (i). While the CNT is biased, the temperature first rises particularly at the CNT contact points on the Au electrodes due to their high resistances, and Au electrodes begin to melt.[6b,23] Upon $F_{electro}$ the

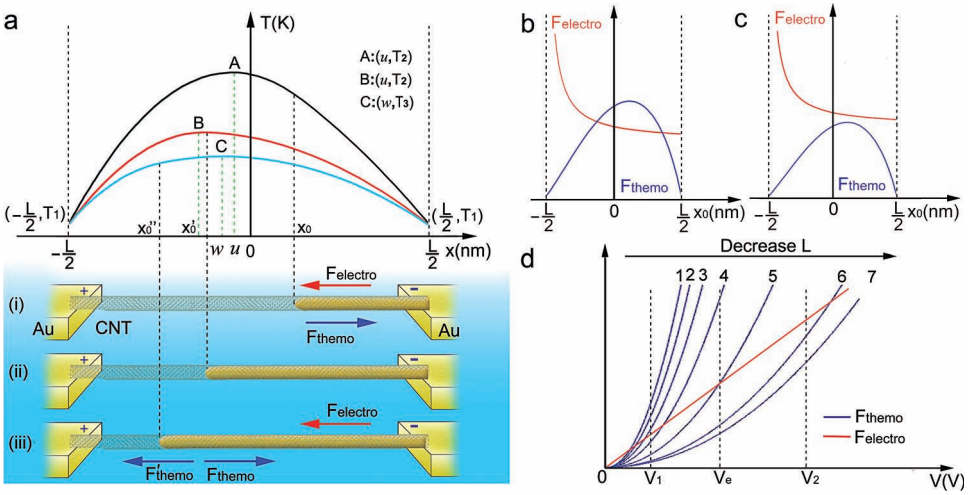

Figure 4. (a) The temperature distribution over the whole CNT combing the Au unfilled and filled sections. The front position of the Au filling from x_0 (black) to x_0' (red) and x_0'' (blue) corresponds to three temperature distribution situations of the whole CNT partly filled with the molten Au, respectively. The lower insets are the schematic diagrams showing two ($F_{electro}$ and F_{thermo}) or three forces ($F_{electro}$, F_{thermo} and F'_{thermo}) imposed on the liquid Au filling in the CNT. (b) and (c) Assuming that an applied voltage is constant, the dynamics simulation curves of $F_{electro}$ (red) and F_{thermo} (blue) are modeled for a long CNT and a short CNT, respectively. (d) Assuming that the applied voltage on the device and the length of the CNT are both variables, the dynamics simulation curves of $F_{electro}$ (red) and F_{thermo} (curves 1–7) are also modeled.

liquid Au flows into the CNT along the direction opposite to the current flow. $F_{electro}$ could be represented as Equation (1) (see method 4 in Supporting Information):

$$F_{electro} = \frac{2k_F e R_0 V_m}{\pi} = \frac{2k_F e R_0 V}{\pi} \frac{\left(\frac{L}{2} - x\right) R_m}{\left(x + \frac{L}{2}\right) R_c + L R_m} \quad (1)$$

where, x_0 is the position of the front of the liquid Au filling in the CNT, L is the length of the CNT, V is the voltage on the CNT, k_F is Fermi wave vector, R_0 is the reflectivity of a scatter, V_m is the voltage on the liquid Au filling part of the CNT, R_m and R_c are the resistivities of the filled Au and the CNT, respectively.

F_{thermo} comes from the momentum transfer from the phonons of the CNT to the liquid Au, driving the material from the hotter place to the colder place. For a two terminal-suspended CNT, assuming symmetric boundary conditions, within a short period the thermal equilibrium can be set up, and its temperature distribution over the whole CNT is applied to parabolic equation.[11,15] But, when the CNT is partly filled with the liquid Au, the temperature distribution along the whole CNT is in different situation, which depends on whether the segment of the CNT is filled with the liquid Au column or not. In this model, it should take thermal conductivities of both the liquid Au filling and the CNT into consideration.[14b,24] It is found that the temperature distribution over the unfilled part of the CNT applied to one parabolic equation, while the temperature distribution along the liquid Au filling part was fit to another parabolic equation. The temperature distribution curves over the whole CNT combining the Au unfilled and filled sections are drawn in Figure 4a. As the length of the liquid Au filling increases, the highest temperature point on the whole CNT will move from the Au unfilled region (u, T_2) (black curve, i; red curve, ii) to the filled region (w, T_3) (blue curve, iii). So, the net force of F_{thermo}-F'_{thermo} on the whole Au filling is always pointed from the front of the Au filling toward the cathode in direction, Figure 4a. The overall F_{thermo} upon the liquid Au filling could be given by Equation (2) (see method 5 in Supporting Information).

$$F_{thermo} = -\frac{\Delta E}{8\pi^2}\left[e^{-\frac{2\Delta E}{k[a(x_0^2-\frac{L^2}{4})+T_1+\frac{a\beta}{L}(x_0-\frac{L}{2})(x_0^2-\frac{L^2}{4})]}} - e^{-\frac{2\Delta E}{kT_1}}\right] \quad (2)$$

where ΔE is barrier height, T_1 is the temperature of both terminals of the CNT, β is weighting factor ($0 < \beta < 1$), and k is the Boltzmann's constant. At a given voltage V on a CNT, $a = -\frac{V^2}{2ARL\kappa}$, where A is the cross section area, R is the resistance, κ is thermal conductivity.

The liquid Au flowing only occurs in a voltage range of $[V_1, V_2]$, where V_1 is defined as the minimum voltage to melt the Au electrodes and V_2 is defined as a critical voltage of the CNT breaking. Assuming the voltage is constant, $F_{electro}$ and F_{thermo} are the functions of x_0 ($-L/2 \le x_0 \le L/2$), and the dynamics simulation curves of $F_{electro}$ and F_{thermo} are shown in Figures 4b and 4c. According to the Equation (2), F_{thermo} will increase when the length of the CNT increases and decrease when the length of the CNT decreases. However, $F_{electro}$ barely changes with the variation of the CNT length. In the beginning, due to a fact that $F_{electro}$ is larger than F_{thermo}, the melted Au easily flows into the CNT along the opposite direction of the current flow. For a long CNT, Figure 4b, when the liquid Au front reaches a specific position inside the CNT, equilibrium between the two forces, i.e., $F_{electro} = F_{thermo}$, comes into effect, resulting in a termination of the Au flow. At this point, the liquid Au nearly freezes and cannot flow from one Au electrode to the other. For a short CNT, Figure 4c, as the maximum of F_{thermo} is smaller than $F_{electro}$, the liquid Au filling flows through this CNT. Notably, as the length of the Au filling increases, F_{thermo} begins to decrease after the maximum due to the decline of temperature gradient; in addition, after the highest temperature point on the whole CNT (w, T_3), the direction of F_{thermo} on the Au filling part between w and L/2 is opposite to F'_{thermo} on the Au filling part between x_0

and w, and this will leads to further decrease of the net force (F_{thermo}-F'_{thermo}) upon the whole Au filling section, while $F_{electro}$ is increasing sharply with the length of the liquid Au filling increases. In this case, the resultant force is getting larger and larger, and the Au melt will be transferred to the opposite Au electrode with an increasing speed, that is, the mass transfer from one electrode to the other is completed.

Furthermore, assuming that the applied voltage on the device and the length of the CNT are both variables, Figure 4d shows the dynamics simulation curves of $F_{electro}$ (red curve) and F_{thermo} (curves 1–7). If the CNT length is known, the required voltage on the device in order to reach an equilibrium can be deduced (*i.e.*, $F_{electro} = F_{thermo}$), which is defined as the equilibrium voltage, V_e, as shown by curve 5. In the first case, when V is smaller than V_e, $F_{electro}$ is larger than F_{thermo}. So, the liquid Au filling can be driven from one Au electrode to the other by uploading a voltage smaller than V_e on the device. In the second case, as the applied voltage is higher than V_e, F_{thermo} will increase drastically, as compared with $F_{electro}$, and F_{thermo} will be significantly larger than $F_{electro}$. As a result, the molten Au starts to dispatch from the CNT along the direction of the current flow. When this bias is increased (to a high value), the liquid Au filling is retracted completely out of the tube, leaving it empty again. Therefore, it is the resultant of the two forces, rather than F_{thermo} or $F_{electro}$ solely, that determines the direction of the melt transport and the position of the molten front inside the CNT. Taken the above discussions together, by simply adjusting the applied voltage and selecting a desired length of the CNT, the liquid Au filling length inside the CNT and the electrical properties of the circuit can be effectively controlled to avoid destroying of the CNT devices.

In conclusion, we present the evidences of a new cause of Joule heating within a simple electronic device involving a multiwalled CNT mounted on two metal electrodes forming an electrical circuit. Though the mass transport for a variety of materials outside or inside the CNTs has been studied,[5–10,18] this time-resolved, high-resolution in-situ observation of metal electrode material melting and its flow driven by a resultant of the thermomigration and electromigration forces through the CNT channel sheds an additional light on the effects affecting the real electrical performance of the CNT-based devices. Melting of electrode materials and their flowing inside CNTs may result in electrical breakdown of the as-established circuit and even a catastrophic failure of the as-made CNT-based devices. In addition, the present finding can inspire us to avoid destroying of the CNT based devices for their reliable electrical performance.

Experimental Section

CNT sample: Multiwalled CNTs were grown by a chemical vapor deposition[13] and see method 6 in Supporting Information.

Transmission electron microscopy: The in-situ microscopy studies were performed in a JEOL 2100F TEM operated at 200 kV. This instrument has a point resolution of 2.4 Å and is equipped with an energy dispersive X-ray detector. Images were taken using a 2 k × 2 k charge-coupled device camera and the Digital Micrograph suite. Videos were recorded using a video-screen grabber when Digital Micrograph was operating in the View mode.

Transmission electron microscope sample holder: Electrical probing and nanomanipulation experiments were carried out with a "Nanofactory Instruments" single-tilt scanning tunneling microscopy-TEM holder. At the beginning of each TEM session, the computer controlling the two-probe set-up was synchronized with the image acquisition workstation. Mechanically cut Au wires and Au tips, 0.25 mm in diameter, were used as electrodes.

Supporting Information

Supporting Information is available from the Wiley Online Library or from the author.

Acknowledgements

This work was financially supported by the National Natural Science Foundation of China (Grant No. 21171035 and 11204030), the Key Grant Project of Chinese Ministry of Education (Grant No. 313015), the Science and Technology Commission of Shanghai-based "Innovation Action Plan" Project (Grant No. 10JC1400100), Shanghai Natural Science Foundation (10ZR1400200), Ph.D. Programs Foundation of Ministry of Education of China (Grant No. 20110075110008), the Fundamental Research Funds for the Central Universities, and the Starting Funding for Youth Teacher in Donghua University.

Received: January 17, 2013
Revised: February 5, 2013
Published online: April 5, 2013

[1] G. F. Close, S. Yasuda, B. Paul, S. Fujita, H. S. P. Wong, *Nano Lett.* **2008**, *8*, 706.
[2] a) J. Li, Q. Ye, A. Cassell, H. T. Ng, R. Stevens, J. Han, M. Meyyappan, *Appl. Phys. Lett.* **2003**, *82*, 2491; b) Y. Awano, S. Sato, D. Kondo, M. Ohfuti, A. Kawabata, M. Nihei, N. Yokoyama, *Phys. Status Solidi A* **2006**, *203*, 3611.
[3] A. Naeemi, J. D. Meindl, *IEEE Electron Dev. Lett.* **2007**, *28*, 135.
[4] a) H. J. Dai, E. W. Wong, C. M. Liebert, *Science* **1996**, *272*, 523; b) P. G. Collins, M. S. Arnold, P. Avouris, *Science* **2001**, *292*, 706.
[5] a) L. X. Dong, X. Y. Tao, L. Zhang, X. B. Zhang, B. J. Nelson, *Nano Lett.* **2007**, *7*, 58; b) D. Golberg, P. M. F. J. Costa, M. Mitome, S. Hampel, D. Haase, C. Mueller, A. Leonhardt, Y. Bando, *Adv. Mater.* **2007**, *19*, 1937.
[6] a) G. E. Begtrup, W. Gannett, T. D. Yuzvinsky, V. H. Crespi, A. Zettl, *Nano Lett.* **2009**, *9*, 1835; b) K. Svensson, H. Olin, E. Olsson, *Phys. Rev. Lett.* **2004**, *93*, 145901; c) J. Zhao, J. Q. Huang, F. Wei, J. Zhu, *Nano Lett.* **2010**, *10*, 4309.
[7] L. X. Dong, X. Y. Tao, M. Hamdi, L. Zhang, X. B. Zhang, A. Ferreira, B. J. Nelson, *Nano Lett.* **2009**, *9*, 210.
[8] M. Löffler, *Adv. Mater.* **2011**, *23*, 541.
[9] P. M. F. J. Costa, D. Golberg, M. Mitome, S. Hampe, A. Leonhardt, B. Buchner, Y. Bando, *Nano Lett.* **2008**, *8*, 3120.
[10] P. M. F. J. Costa, U. K. Gautam, Y. Bando, D. Golberg, *Nat. Commun.* **2011**, *2*, 421.
[11] a) B. M. Kim, S. Sinha, H. H. Bau, *Nano Lett.* **2005**, *5*, 873; b) D. Schebarchov, S. C. Hendy, *Nano Lett.* **2008**, *8*, 2253.
[12] a) D. G. Pierce, P. G. Brusius, *Microelectron. Reliab.* **1997**, *37*, 1053; b) P. G. Collins, M. Hersam, M. Arnold, R. Martel, P. Avouris, *Phys. Rev. Lett.* **2001**, *86*, 3128.
[13] J. Q. Hu, Y. Bando, J. H. Zhan, C. Y. Zhi, F. F. Xu, D. Golberg, *Adv. Mater.* **2006**, *18*, 197.
[14] a) K. H. Baloch, N. Voskanian, M. Bronsgeest, J. Cumings, *Nat. Nanotechnol.* **2012**, *7*, 316; b) G. E. Begtrup, K. G. Ray, B. M. Kessler, T. D. Yuzvinsky, H. Garcia, A. Zettl, *Phys. Rev. Lett.* **2007**, *99*, 155901.

[15] A. Barreiro, R. Rurali, E. R. Hernandez, J. Moser, T. Pichler, L. Forro, A. Bachtold, *Science* **2008**, *320*, 775.
[16] a) M. S. Wang, J. Y. Wang, Q. Chen, L. M. Peng, *Adv. Funct. Mater.* **2005**, *15*, 1825; b) P. Singjai, S. Changsarn, S. Thongtem, *Mater. Sci. Eng. A* **2007**, *443*, 42; c) J. A. Rodríguez-Manzo, M. S. Wang, F. Banhart, Y. Bando, D. Golberg, *Adv. Mater.* **2009**, *21*, 1; d) M. S. Wang, D. Golberg, Y. Bando, *Adv. Mater.* **2010**, *22*, 93.
[17] P. S. Dorozhkin, S. V. Tovstonog, D. Golberg, J. H. Zhan, Y. Ishikawa, M. Shiozawa, H. Nakanishi, K. Nakata, Y. Bando, *Small* **2005**, *1*, 1088.
[18] a) B. C. Regan, S. Aloni1, R. O. Ritchie, U. Dahmen, A. Zettl, *Nature* **2004**, *428*, 924; b) C. H. Jin, K. Suenaga, S. Iijima, *Nat. Nanotechnol.* **2008**, *3*, 17; c) J. A. Rodríguez-Manzo, M. Terrones, H. Terrones, H. W. Kroto, L. T. Sun, F. Banhart, *Nat. Nanotechnol.* **2007**, *2*, 307.
[19] a) M. Whitby, N. Quirke, *Nat. Nanotechnol.* **2007**, *2*, 87; b) X. J. Gong, J. Y. Li, H. J. Lu, R. Z. Wan, J. C. Li, J. Hu, H. P. Fang, *Nat. Nanotechnol.* **2007**, *2*, 709.
[20] R. S. Sorbello, *Solid State Phys.* **1998**, *51*, 159.
[21] a) P. M. Ajayan, S. Iijima, *Nature* **1993**, *361*, 333; b) J. Y. Chen, A. Kutana, C. P. Collier, K. P. Giapis, *Science* **2005**, *310*, 1480.
[22] Y. S. Chen, Y. C. Chang, S. C. Wang, L. Y. Chen, D. H. Lien, L. J. Chen, C. S. Chang, *Small* **2012**, *8*, 2158.
[23] a) R. S. Sorbello, *Phys. Rev. B* **1989**, *39*, 4984; b) S. Heinze, N. P. Wang, J. Tersoff, *Phys. Rev. Lett.* **2005**, *95*, 186802.
[24] G. Pottlacher, *J. Non-Cryst. Solids* **1999**, *250-252*, 177.